

## Enhancing the stability of microplasma device utilizing diamond coated carbon nanotubes as cathode materials

Tingsun Chang, Srinivasu Kunuku, Kamatchi Jothiramalingam Sankaran, Keh-Chyang Leou, Nyanhwa Tai, and I-Nan Lin

Citation: [Applied Physics Letters](#) **104**, 223106 (2014); doi: 10.1063/1.4881419

View online: <http://dx.doi.org/10.1063/1.4881419>

View Table of Contents: <http://scitation.aip.org/content/aip/journal/apl/104/22?ver=pdfcov>

Published by the [AIP Publishing](#)

---

### Articles you may be interested in

[High stability electron field emitters made of nanocrystalline diamond coated carbon nanotubes](#)

Appl. Phys. Lett. **103**, 251601 (2013); 10.1063/1.4850525

[Microplasma enhancement via the formation of a graphite-like phase on diamond cathodes](#)

J. Vac. Sci. Technol. B **31**, 02B108 (2013); 10.1116/1.4769373

[Materials characteristics and surface morphology of a cesium iodide coated carbon velvet cathode](#)

J. Appl. Phys. **103**, 013302 (2008); 10.1063/1.2821152

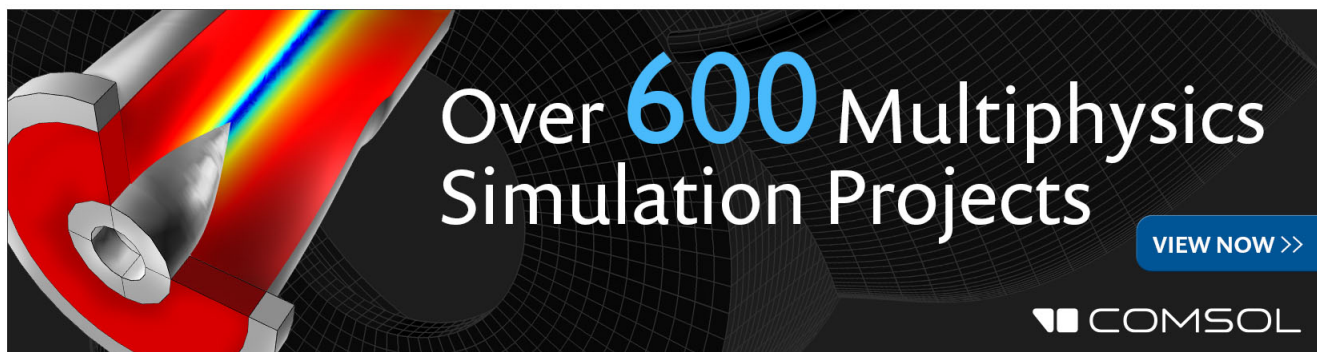
[Plasma illumination devices enhanced by carbon nanotubes](#)

Appl. Phys. Lett. **88**, 013104 (2006); 10.1063/1.2158153

[Carbon nanotube-enhanced performance of microplasma devices](#)

Appl. Phys. Lett. **84**, 4481 (2004); 10.1063/1.1755845

---

The advertisement features a dark background with a grid pattern. On the left, there is a 3D simulation of a mechanical part with a red and yellow color gradient. The text 'Over 600 Multiphysics Simulation Projects' is prominently displayed in the center. To the right of the text is a blue button with the text 'VIEW NOW >>'. In the bottom right corner, the COMSOL logo is visible, consisting of a small square icon followed by the word 'COMSOL'.

# Enhancing the stability of microplasma device utilizing diamond coated carbon nanotubes as cathode materials

Tingsun Chang,<sup>1</sup> Srinivasu Kunuku,<sup>2</sup> Kamatchi Jothiramalingam Sankaran,<sup>1</sup> Keh-Chyang Leou,<sup>2</sup> Nyanhwa Tai,<sup>1,a)</sup> and I-Nan Lin<sup>3,a)</sup>

<sup>1</sup>Department of Materials Science and Engineering, National Tsing-Hua University, Hsinchu 300, Taiwan

<sup>2</sup>Department of Engineering and System Science, National Tsing-Hua University, Hsinchu 300, Taiwan

<sup>3</sup>Department of Physics, Tamkang University, Tamsui 251, Taiwan

(Received 3 April 2014; accepted 22 May 2014; published online 4 June 2014)

This paper reports the enhanced stability of a microplasma device by using hybrid-granular-structured diamond (HiD) film coated carbon nanotubes (CNTs) as cathode, which overcomes the drawback of short life time in the CNTs-based one. The microplasma device can be operated more than 210 min without showing any sign of degradation, whereas the CNTs-based one can last only 50 min. Besides the high robustness against the Ar-ion bombardment, the HiD/CNTs material also possesses superior electron field emission properties with low turn-on field of 3.2 V/ $\mu\text{m}$ , which is considered as the prime factor for the improved plasma illumination performance of the devices. © 2014 AIP Publishing LLC. [<http://dx.doi.org/10.1063/1.4881419>]

Microplasma has attracted much attention owing to several advantageous characteristics, including low power consumption, relatively high electron density, and high electron temperature.<sup>1</sup> Microplasma has found potential applications in many areas such as environmental remediation,<sup>2</sup> biology and biomedicine,<sup>3</sup> intense light source in the vacuum ultraviolet,<sup>4–6</sup> gas surface analysis, ion source for spectrometry, and mass spectrometry.<sup>7–9</sup> In a conventional gas discharge, the natural radiation background, such as cosmic rays, can initiate efficiently the breakdown process for the plasma. However, the probability of plasma ignition due to natural radiation decreases proportionally with the discharge volume and becomes inefficient for microplasma. Intentional injection of electrons has thus been attempted to decrease the breakdown voltage in microplasma. Field emission materials, such as carbon nanotubes (CNTs), have been demonstrated to reduce the ignition voltages by 14%–18% in microplasma devices.<sup>10–12</sup> However, the short lifetime and the poor stability of the CNTs emitters, especially in a plasma environment, have been the major barriers averting their profitable viability.<sup>13,14</sup> To surmount this drawback, CNTs have been combined with other field emitting materials by depositing thin films on CNTs,<sup>15–17</sup> decorating CNTs with nanoparticles,<sup>18</sup> or by making composites of CNTs.<sup>19,20</sup>

On the other hand, diamond has the most strongly bonded crystal structure and has excellent physical and chemical properties, which makes it a potential electron source with higher lifetime and reliability. It is interesting to integrate the high robustness of diamond films and marvelous electron field emission (EFE) properties of CNTs to yield highly stable electron sources. Actually, many attempts have been made to couple the diamond and CNTs,<sup>16,17,21–24</sup> but the results are still not satisfactory that is probably due to the difficulty in integration of the two materials. Moreover, among the diamond films developed for EFE applications, the ones with hybrid granular structure, the HiD films, which

were obtained by growing the nanocrystalline diamond (NCD) on ultrananocrystalline diamond (UNCD) seeding layer, possess marvelous EFE properties<sup>25,26</sup> and are most appropriate for the development of diamond-CNTs composite EFE emitters for microplasma applications.

In this present work, the HiD films were synthesized on CNTs using a two-step microwave plasma enhanced chemical vapor deposition (MPE-CVD) process. These synthesized high EFE materials were utilized as cathode for fabricating microplasma device and their plasma illumination (PI) behavior was also investigated. Markedly, enhanced lifetime stability for the microplasma devices has been achieved and the improvement in the PI behavior for the microplasma devices was intimately correlated to the EFE behavior of the cathode materials. The possible mechanism for such a phenomenon was discussed.

The CNTs were grown on Si substrates, using  $\text{C}_2\text{H}_2$  as carbon sources and Fe nanoclusters as catalysts in a thermal chemical vapor deposition process (750 °C, 10 min). The Fe nanoclusters were formed by the rapid thermal annealing (750 °C, 5 min) of a thin Fe coating ( $\sim 1$  nm) on Si substrates, which contain  $8\ \mu\text{m} \times 8\ \mu\text{m}$  square patterns ( $8\ \mu\text{m}$  in separation). The CNTs patterns were grown thermally in 10% $\text{H}_2$ /Ar environment (10 Torr) at 750 °C for 10 min after 10 sccm  $\text{C}_2\text{H}_2$  was fed into the furnace. Figure 1(a) shows the cross-sectional SEM morphology of the CNTs used for growing the diamond films, whereas the inset I in this figure shows the top-view SEM micrograph of the CNTs.

Prior to the growth of diamond films, the CNTs were first coated with a thin layer of Au ( $\sim 10$  nm). Direct synthesis of diamond films on CNTs is quite difficult. When the Au-coated CNTs were loaded in a MPE-CVD system for growing the UNCD films, CNTs were completely etched out by the  $\text{CH}_4$ /Ar plasma. No diamond films can be grown directly on top of CNTs. To solve the difficulty in growing diamond on CNTs by MPE-CVD process, electrophoresis deposition process<sup>27</sup> was utilized to precoat nano-diamond particulates ( $\sim 10$  nm in size) on the tip of CNTs to protect them from Ar ions bombardment damage. The UNCD films were first grown

<sup>a)</sup>Authors to whom correspondence should be addressed. Electronic addresses: nhtai@mx.nthu.edu.tw and inanlin@mail.tku.edu.tw

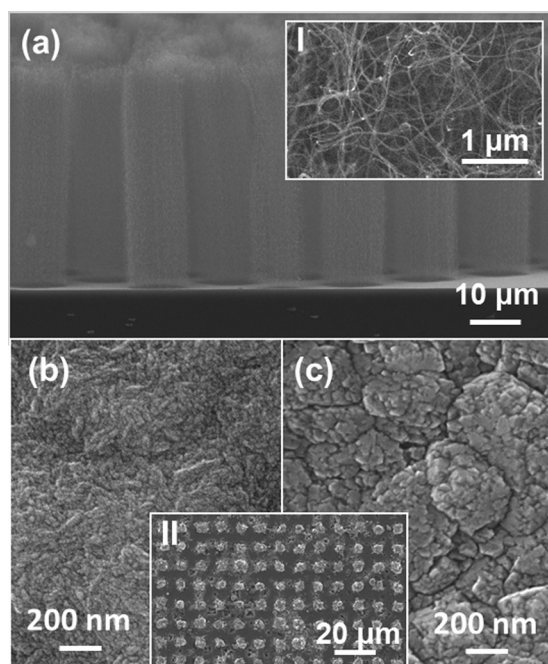


FIG. 1. (a) The cross-sectional SEM micrographs of the vertically align CNTs grown on Si-substrates (the CNTs are about  $34\ \mu\text{m}$  in length) with the inset I showing the top-view SEM micrographs of the CNTs. The SEM micrographs of the (b) UNCD/Au/CNTs and (c) HiD/Au/CNTs films with the inset II showing the EFE emission array made of diamond coated CNTs. The UNCD films were grown using  $\text{CH}_4(4\%)/\text{Ar}$  plasma, whereas the HiD films were grown on top of the UNCD/Au/CNTs films using  $\text{CH}_4(1\%)/\text{Ar}(49\%)/\text{H}_2(50\%)$  plasma.

on the nano-diamond decorated Au-CNTs by using MPE-CVD system (2.45 GHz, IPLAS-CYRANNUS) in a  $\text{CH}_4(4\%)/\text{Ar}$  plasma with a microwave power of 1200 W for 60 min. The pressure and the total flow rate were maintained at 120 Torr and 100 sccm, respectively. The decoration of nano-diamond particulates on CNTs not only increased the durability of CNTs in  $\text{CH}_4/\text{Ar}$  plasma but also facilitated markedly the nucleation of diamond. However, the nucleation and growth behavior of UNCD films on nano-diamond decorated CNTs is very much different from that on planar Si-substrates. No diamond films can be grown on top of CNTs, when the  $\text{CH}_4$ -content in the  $\text{CH}_4/\text{Ar}$  plasma is smaller than 4%. Only when the  $\text{CH}_4$ -content in the plasma is larger than such a critical value, the UNCD films can grow nicely, fully covering the CNTs. No external heater was used to heat the substrate. The substrate temperature was increased due to the plasma bombardment heating upto around  $450^\circ\text{C}$ , which was monitored by a thermocouple embedded in the stainless steel substrate holder. Figure 1(b) shows that the morphology of the UNCD films grown on top of nano-diamond decorated CNTs is similar to those of the conventional UNCD films grown on Si-substrates, i.e., they contain nano-sized diamond grains with very smooth surface. The inset II in this figure shows the top-view SEM micrograph of the UNCD coated CNTs patterns.

After successful growth of UNCD films on CNTs, the growth of HiD films by the subsequent MPE-CVD process using  $\text{CH}_4(1\%)/\text{Ar}(49\%)/\text{H}_2(50\%)$  plasma is straightforward. Notably, the purpose of secondary MPE-CVD process is to modify the granular structure of UNCD layer, as previous studies<sup>25,26</sup> indicated that such a secondary MPE-CVD process will

preferentially etch out the transpolyacetylene phase in the grain boundaries, trigger the coalescence of the nano-sized diamond grains, and induce the formation of nano-graphitic clusters. Such a two-step MPE-CVD process formed a hybrid granular structured diamond films with superior EFE properties, which is even better than that of the UNCD films. The typical SEM morphology of the HiD/Au/CNTs films is shown in Fig. 1(c), indicating the formation of cauliflower-like morphology with the size around 100 nm.

To investigate the PI characteristics of microplasma device, bare or diamond coated CNTs were utilized as cathode and the indium tin oxide (ITO) coated glass as anode. The cathode-to-anode separation was fixed by a polytetrafluoroethylene (PTFE) spacer (1.0 mm in thickness). A circular hole about 3.0 mm in diameter was cut out from the PTFE spacer to form a microcavity. The plasma was triggered using a pulsed direct current voltage in a bipolar pulse mode (20 ms square pulse, 6 kHz repetition rate). The chamber was evacuated to reach a base pressure of 0.1 mTorr and then purged with Ar for 10 min (in 2 Torr). The Ar gas was channeled into the chamber at a flow rate of 10 sccm throughout the measurements. The plasma current versus applied voltage was measured using an electrometer (Keithley 237). Typical plasma images for the microplasma devices excited by 540 V were illustrated as insets in Fig. 2(a). The microplasma devices using bare or diamond

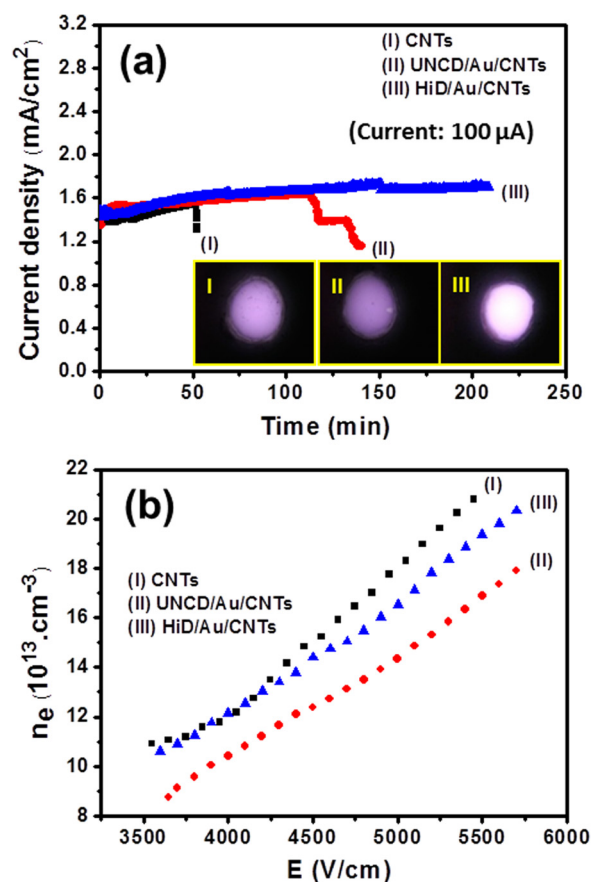


FIG. 2. The (a) lifetime and (b) the plasma density vs. applied field ( $n_e$ -E) characteristics of the microplasma devices using (I) CNTs, (II) UNCD/Au/CNTs and (III) HiD/Au/CNTs films as cathode. The insets in "a" show the typical plasma illumination images of the microplasma devices. The UNCD films were grown using  $\text{CH}_4(4\%)/\text{Ar}$  plasma, whereas the HiD films were grown on top of the UNCD/Au/CNTs films using  $\text{CH}_4(1\%)/\text{Ar}(49\%)/\text{H}_2(50\%)$  plasma.



coated CNTs as cathode can be ignited at a low voltage as 360 V, which corresponds to threshold field as  $(E_{\text{pl}})_{\text{CNT}} = 3600 \text{ V/cm}$ , regardless of the cathode materials. The brightness of the plasma increased monotonically with the applied voltage (not shown). The plasma illumination characteristic of the microplasma devices is better illustrated by the applied field dependence of the plasma current density (not shown). For the CNTs based microplasma devices, the plasma current density ( $J_{\text{pl}}$ ) increased from  $(J_{\text{pl}}) = 1.28 \text{ mA/cm}^2$  at an applied field of 3600 V/cm to around  $2.5 \text{ mA/cm}^2$  at 5500 V/cm. In contrast, the UNCD/Au/CNTs based microplasma devices possess smaller plasma current density [ $(J_{\text{pl}})_{\text{UNCD}} = 1.92 \text{ mA/cm}^2$  at 5500 V/cm], compared with those for the CNTs based devices. However, these PI behaviors are still better than those of UNCD/Si films [ $(J_{\text{pl}})_{\text{UNCD/Si}} = 1.37 \text{ mA/cm}^2$  at 5500 V/cm] based devices.

From each  $(J_e)_{\text{pl}}$  value, we can calculate the plasma density, which is the same as the electron density ( $n_e$ ) for the plasma, by using Eqs. (1)–(3)<sup>28</sup>

$$n_e = \frac{J}{E\mu_e e}. \quad (1)$$

Here,  $J$  is the plasma current density,  $E$  is the applied electric field,  $e$  is the electron charge, and  $\mu_e$  is the electron mobility, which can be calculated by the Einstein relation

$$\frac{D}{\mu} = \frac{kT}{e}. \quad (2)$$

Here,  $k$  is the Boltzmann constant,  $T_e$  is the electron temperature, and  $D$  is the diffusion coefficient, which can be estimated from the empirical formula

$$D = \frac{K \times 10^5}{p}. \quad (3)$$

Here,  $p$  is the pressure and  $K$  value is 6.3 for Ar gas.<sup>28</sup> By using computational fluid dynamics (CFD) simulations, we have estimated  $T_e = 2 \text{ eV}$  for pressure of 2–100 Torr. Figure 2(b) shows that, for the CNTs based microplasma devices, the plasma density ( $n_e$ ) increased monotonously against the applied field, reaching a value of  $(n_e)_{\text{CNT}} = 2.1 \times 10^{14} \text{ cm}^{-3}$  at an applied field of 5500 V/cm. Similarly, by using Eqs. (1)–(3), we calculated the plasma density,  $n_e$ , out of the

corresponding  $J_{\text{pl}}$ -value for the UNCD/Au/CNTs based microplasma devices and the  $n_e$ - $E$  curves are shown as curve II in Fig. 2(b), revealing that the  $n_e$ -values reach around  $\sim 1.7 \times 10^{14} \text{ cm}^{-3}$  at an applied field of 5500 V/cm, which is smaller than that of the CNTs-based microplasma devices. These PI characteristics were summarized in Table I.

Even though the CNTs-based microplasma devices own superior PI behavior to those based on UNCD/Au/CNTs cathode, they suffer from short lifetime. Curve I in Fig. 2(a) indicates that the microplasma devices using CNT as cathodes can last only for 50 min when tested in  $1.41 \text{ mA/cm}^2$  ( $100 \mu\text{A}$ , Ar, 10 Torr). In contrast, curve II in Fig. 2(a) shows that, although the UNCD/Au/CNTs based microplasma devices do not show as good PI properties as that of the CNTs based ones, these devices can be operated at the same conditions for more than  $(\tau_{\text{pl}})_{\text{UNCD}} = 110 \text{ min}$  before starting to decay, which is overwhelmingly superior to the CNT-based microplasma devices.

Using HiD films to replace for the UNCD films in diamond-CNTs materials markedly improved the PI behavior of the microplasma devices. The plasma current density attained a large value as  $(J_{\text{pl}})_{\text{HiD/CNTs}} = 2.23 \text{ mA/cm}^2$  at an applied field of 5500 V/cm (not shown). Moreover, the plasma density reached a large value,  $(n_e)_{\text{HiD/CNTs}} = 1.95 \times 10^{14} \text{ cm}^{-3}$  at an applied field of 5500 V/cm (curve III, Fig. 2(b)). These behaviors are markedly better than those for the microplasma devices using UNCD/Au/CNTs as cathode. Intriguingly, utilizing HiD/Au/CNTs to replace for the UNCD/Au/CNTs as cathode in the microplasma devices can not only attain larger plasma density but also reached markedly better durability for the devices. Curve III in Fig. 2(a) shows that the microplasma devices using HiD/Au/CNTs materials as cathode can last more than  $(\tau_{\text{pl}})_{\text{HiD}} = 210 \text{ min}$  when operated at the same conditions, i.e.,  $1.41 \text{ mA/cm}^2$ , before showing the sign of decaying that is superior to the UNCD-based microplasma devices.

To investigate how the PI behavior of a microplasma device is correlated with the EFE properties of the cathode materials, the EFE properties of the bare and diamond coated CNTs were measured with a parallel plate setup, in which the cathode was bare CNTs (or diamond-coated CNTs) and the anode was phosphor coated onto an ITO coated glass. The cathode-to-anode distance was fixed constant by a PTFE spacer with a thickness of  $200 \mu\text{m}$ . The current-voltage ( $I$ - $V$ )

TABLE I. The EFE and PI characteristics of CNTs, UNCDn/CNTs, and HiD/CNTs composite materials.

Materials	Plasma performance				EFE properties		
	$(E_{\text{th}})_{\text{pl}}^{\text{a}}$ (V/ $\mu\text{m}$ )	$J_{\text{pl}}^{\text{b}}$ (mA/cm <sup>2</sup> )	$n_e^{\text{c}}$ ( $10^{14} \text{ cm}^{-3}$ )	$\tau_{\text{pl}}^{\text{d}}$ (min)	$E_0^{\text{e}}$ (V/ $\mu\text{m}$ )	$J_e^{\text{f}}$ (mA/cm <sup>2</sup> )	$\tau_{\text{efe}}^{\text{g}}$ (min)
CNTs	0.36	2.45	2.10	50	0.70	4.83@1.08	30@400 V
UNCD/Au/CNTs	0.36	1.92	1.68	110	4.00	0.16@4.88	270@1000 V
HiD/Au/CNTs	0.36	2.24	1.95	210	3.20	1.83@4.88	420@1000 V

<sup>a</sup> $(E_{\text{th}})_{\text{pl}}$ : the threshold field for igniting the plasma in parallel-plate microplasma devices.

<sup>b</sup> $J_{\text{pl}}$ : the plasma current density in parallel-plate microplasma devices measured at an applied field of 0.55 V/ $\mu\text{m}$ .

<sup>c</sup> $n_e$ : the plasma density, which is also the electron density in the parallel-plate microplasma devices, measured at an applied field of 0.55 V/ $\mu\text{m}$ .

<sup>d</sup> $\tau_{\text{pl}}$ : the life time measured at  $100 \mu\text{A}$  ( $1.41 \text{ mA/cm}^2$ ) applied current in parallel-plate microplasma devices.

<sup>e</sup> $E_0$ : the turn-on field for inducing EFE process, which was designated as the interception of the straight line segments extrapolated from the low-field and high field of FN plots.

<sup>f</sup> $J_e$ : the EFE current density at the designated applied field in V/ $\mu\text{m}$ .

<sup>g</sup> $\tau_{\text{efe}}$ : the life time measured at the designated applied voltage.

characteristics were measured using an electrometer (Keithley 2410) under pressure below  $10^{-6}$  Torr and were modelled by Fowler-Nordheim theory.<sup>29</sup> The CNTs possess very good EFE properties. Curve I in Fig. 3(a) shows that the EFE process for CNTs can be turned on at  $(E_0)_{\text{CNT}} = 0.70 \text{ V}/\mu\text{m}$  and the EFE current density reached a large value,  $(J_e)_{\text{CNT}} = 4.83 \text{ mA}/\text{cm}^2$  at an applied field of  $1.08 \text{ V}/\mu\text{m}$ . In contrast, curve II in Fig. 3(a) shows that the EFE process for UNCD/Au/CNTs films can be turned on at  $(E_0)_{\text{UNCD}} = 4.0 \text{ V}/\mu\text{m}$ , attaining a large EFE current density of  $(J_e)_{\text{UNCD}} = 1.6 \text{ mA}/\text{cm}^2$  at an applied field of  $5.98 \text{ V}/\mu\text{m}$ . Although these EFE properties are inferior to those of CNTs emitters, they are markedly better than the UNCD films grown directly on Si-substrates [ $(E_0)_{\text{UNCD/Si}} = 16.86 \text{ V}/\mu\text{m}$  and  $(J_e)_{\text{UNCD/Si}} = 0.002 \text{ mA}/\text{cm}^2$  at  $7.0 \text{ V}/\mu\text{m}$ ]. Moreover, using HiD films to replace for the UNCD films in diamond-CNTs materials markedly improved their EFE behavior of the composite materials. Curve III in Figure 3(a) shows that the EFE process of the HiD/Au/CNTs films can be turned on at  $(E_0)_{\text{HiD}} = 3.20 \text{ V}/\mu\text{m}$ , achieving a large EFE current density of  $(J_e)_{\text{HiD}} = 1.83 \text{ mA}/\text{cm}^2$  at an applied field of  $4.88 \text{ V}/\mu\text{m}$  that is much better than those for UNCD/Au/CNTs films (cf. Table I).

Even though the CNTs own overwhelmingly superior EFE properties, they suffer from short lifetime. Figure 3(b)

(curve I) shows that the lifetime of CNTs EFE emitters is as short as  $\tau_{\text{CNTs}} = 30 \text{ min}$  when tested under  $400 \text{ V}$  in  $10^{-6}$  Torr. In contrast, the UNCD/Au/CNTs emitters exhibit markedly longer lifetime compared with those based on CNTs. Curve II in this figure reveals that the UNCD/Au/CNTs emitters can last more than  $\tau_{\text{UNCD}} = 270 \text{ min}$  without showing any sign of degradation when tested at applied voltage of  $1000 \text{ V}$ . What is intriguing is that the conversion of UNCD films into HiD films in diamond-coated CNTs emitters not only enhanced the EFE properties of the emitters but also improved the robustness of these devices. Curve III of Fig. 3(b) shows that the lifetime of HiD/Au/CNTs emitters is around  $\tau_{\text{HiD}} = 420 \text{ min}$  when tested at the same conditions. The insets in Fig. 3(b) show the typical EFE images. Notably, the UNCD/Au/CNTs emitters possessed superior EFE properties, as compared with the UNCD films coated on CNTs without using the Au-interlayer<sup>30</sup> and thus resulted in better PI performance of the microplasma device using these materials as cathode. Moreover, HiD/Au/CNTs emitters possess much better EFE and PI characteristics than the HiD/CNTs.<sup>31</sup> How the presence of Au-interlayer between the diamond and CNTs can markedly enhance the EFE and PI behavior is still not clear. The possible reason may be that the Au-coating forms as nanodots sit on the tip of CNTs, which improves the adhesion of nano-sized diamond particulates, and therefore facilitates the formation of diamond nuclei on top of the CNTs.

The PI and EFE processes seem to be two irrelevant phenomena and the reason for better plasma illumination performance on using the cathode material with superior EFE properties cannot be explained in a straightforward way. It should be mentioned that the threshold field,  $(E_{\text{th}})_{\text{pl}}$ , required to trigger the Ar plasma for the microplasma devices using diamond as cathodes is perceptibly smaller than the turn-on field,  $(E_0)_{\text{efe}}$ , for inducing the EFE process of the corresponding HiD/Au/CNTs diamond films (cf. Table I,  $(E_{\text{th}})_{\text{pl}} = 0.36 \text{ V}/\mu\text{m}$  and  $(E_0)_{\text{efe}} = 3.20 \text{ V}/\mu\text{m}$ ). Such a phenomenon is due to the difference in the mechanism for igniting the plasma in Ar environment (tens of Torr) and that for turning on the EFE process in high vacuum environment ( $10^{-6}$  Torr). In a microplasma device, the plasma can be triggered when the “secondary electrons” emitted from the cathode gain sufficient kinetic energy to ionize the gas molecules (e.g.,  $15.7 \text{ eV}$  for Ar-species). Before the onset of plasma, the electric field imposed on the cathode materials is far below the turn-on field needed for inducing the EFE process. Only the secondary electrons contribute to the ionization of Ar-gas molecules. Therefore, it seems that the low EFE turn-on field for the HiD/Au/CNTs films is not helpful in lowering the threshold field for igniting the plasma compared with those for UNCD/Au/CNTs ones. However, when the plasma was ignited, there formed a plasma sheath in the vicinity of cathode, where the electric field will be markedly increased. For typical plasma with the sheath around  $10 \mu\text{m}$  in thickness, the electric field experienced by the cathode will increase to around  $36.0 \text{ V}/\mu\text{m}$  for an applied voltage of  $360 \text{ V}$ . Such a field is far larger than that necessary for turning on the EFE process for most of the diamond films. Large number of electrons will be emitted from the diamond cathode material, which increases the cascading ionization of the

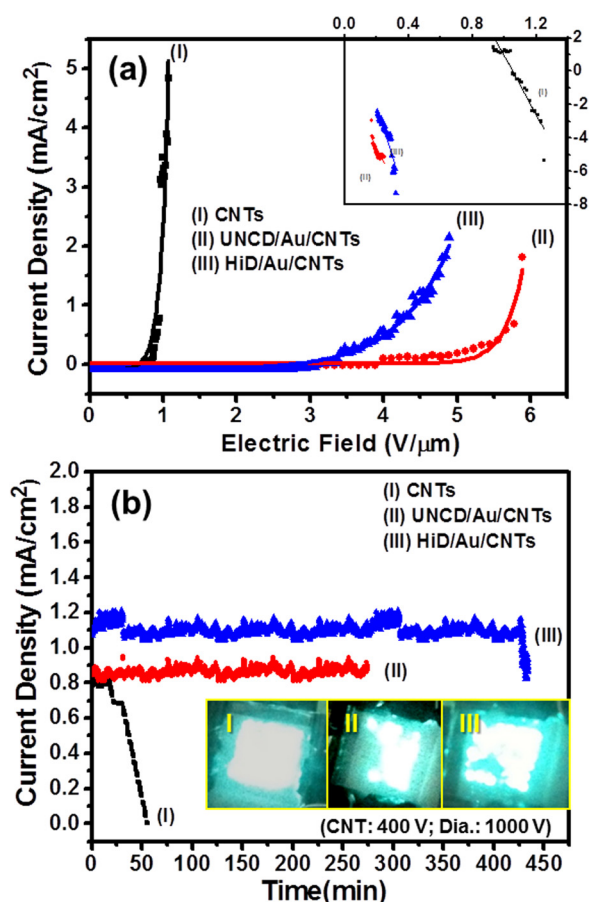


FIG. 3. The (a) electron field emission properties, J-E curves, and (b) EFE life time of (I) CNTs, (II) UNCD/Au/CNTs, and (III) HiD/Au/CNTs emitters. The inset in “a” shows the Fowler-Nordheim plot of the J-E curve and the insets in “b” show the typical images of the EFE devices. The UNCD films were grown using  $\text{CH}_4(4\%)/\text{Ar}$  plasma, whereas the HiD films were grown on top of the UNCD/Au/CNTs films using  $\text{CH}_4(1\%)/\text{Ar}(49\%)/\text{H}_2(50\%)$  plasma.

Ar gas molecules and increases noticeably the plasma density. Therefore, larger  $J_{\text{pl}}$  and  $n_e$  were observed for the microplasma when the HiD/Au/CNTs films were used as cathodes, compared with those used UNCD/Au/CNTs as cathode (cf. Table I).

In summary, a facile and reproducible way of synthesizing HiD films on CNTs with long lifetime stability PI performances, overcoming the poor stability problems of CNTs based microplasma devices has been demonstrated. The plasma current of 100  $\mu\text{A}$  (1.41  $\text{mA}/\text{cm}^2$ ) was upheld for a period over 210 (or 110) min, showing better plasma stability for HiD (or UNCD) based microplasma devices, compared with that of bare CNTs ( $(\tau_{\text{pl}})_{\text{CNTs}} = 50$  min). In addition, the HiD/Au/CNTs (or UNCD/Au/CNTs) emitters exhibit excellent EFE life-time stability of  $(\tau_{\text{efe}})_{\text{diamond}} = 420$  (or 270 min), when tested at applied voltage of 1000 V, whereas that of the CNTs emitters is only  $(\tau_{\text{efe}})_{\text{CNTs}} = 30$  min at applied voltage of 400 V. The present approach of synthesizing HiD materials is a direct and simple process that provides a solution for the fabrication of functional microplasma devices.

The authors would like to thank the National Science Council, Taiwan, Republic of China, for the support of this research through the Project Nos. NSC102-2112-M032-006 and NSC 101-2221-E-007-064-MY3.

- <sup>1</sup>K. H. Becker, K. H. Schoenbach, and J. G. Eden, *J. Phys. D: Appl. Phys.* **39**, R55 (2006).
- <sup>2</sup>T. Tomai, K. Katahira, H. Kubo, Y. Shimizu, T. Sasaki, N. Koshizaki, and K. Terashima, *J. Supercrit. Fluids* **41**, 404 (2007).
- <sup>3</sup>J. A. Pérez-Martínez, R. Peña-Eguiluz, R. López-Callejas, A. Mercado-Cabrera, R. A. Valencia, S. R. Barocio, J. S. Benítez-Read, and J. O. Pacheco-Sotelo, *Surf. Coat. Technol.* **201**, 5684 (2007).
- <sup>4</sup>S. J. Park, K. S. Kim, and J. G. Eden, *J. Appl. Phys.* **99**, 026107 (2006).
- <sup>5</sup>S. J. Park, J. D. Readle, A. J. Price, J. K. Yoon, and J. G. Eden, *J. Phys. D: Appl. Phys.* **40**, 3907 (2007).
- <sup>6</sup>U. Kogelschatz, *J. Opt. Technol.* **79**(8), 484 (2012).
- <sup>7</sup>R. Guchardi and P. C. Hauser, *J. Chromatogr. A* **1033**, 333 (2004).
- <sup>8</sup>Y. Hozumi, T. Seto, M. Hirasawa, M. Tsuji, and A. Okuyama, *J. Electrostat.* **67**, 1 (2009).

- <sup>9</sup>A. Michels, S. Tombrink, W. Vautz, M. Miclea, and J. Franzke, *Spectrochim. Acta, Part B* **62**, 1208 (2007).
- <sup>10</sup>S. J. Park, J. G. Eden, and K.-H. Park, *Appl. Phys. Lett.* **84**, 4481 (2004).
- <sup>11</sup>S. J. Park and J. G. Eden, *Electron. Lett.* **39**, 773 (2003).
- <sup>12</sup>J. G. Eden, S. J. Park, N. P. Ostrom, and K. F. Chen, *J. Phys. D: Appl. Phys.* **38**, 1644 (2005).
- <sup>13</sup>K. A. Dean, T. P. Burgin, and B. R. Chalamala, *Appl. Phys. Lett.* **79**, 1873 (2001).
- <sup>14</sup>J. M. Green, L. Dong, T. Gutu, J. Jiao, J. F. Conley, and J. Y. Ono, *J. Appl. Phys.* **99**, 094308 (2006).
- <sup>15</sup>H. Sharma, V. Kaushik, P. Girdhar, V. N. Singh, A. K. Shukla, and V. D. Vankar, *Thin Solid Films* **518**, 6915 (2010).
- <sup>16</sup>Y. Zou, P. W. May, S. M. C. Vieira, and N. A. Fox, *J. Appl. Phys.* **112**, 044903 (2012).
- <sup>17</sup>A. Fiori, S. Orlanducci, V. Sessa, E. Tamburri, F. Toschi, M. L. Terranova, A. Ciorba, M. Rossi, M. Lucci, and A. S. Barnard, *J. Nanosci. Nanotechnol.* **8**, 1989 (2008).
- <sup>18</sup>D. H. Lee, J. A. Lee, W. J. Lee, D. S. Choi, W. J. Lee, and S. O. Kim, *J. Phys. Chem. C* **114**, 21184 (2010).
- <sup>19</sup>J. M. Rosolen, S. Tronto, M. S. Marchesin, E. C. Almeida, N. G. Ferreira, C. H. Patrick Poá, and S. R. P. Silva, *Appl. Phys. Lett.* **88**, 083116 (2006).
- <sup>20</sup>D. Varshney, M. Ahmadi, M. J. F. Guinel, B. R. Weiner, and G. Morell, *Nanoscale Res. Lett.* **7**, 535 (2012).
- <sup>21</sup>V. K. Rangari, G. M. Mohammad, S. Jeelani, Y. V. Butenko, and V. R. Dhanak, *ACS Appl. Mater. Interfaces* **2**, 1829 (2010).
- <sup>22</sup>L. T. Sun, J. L. Gong, Z. Y. Zhu, D. Z. Zhu, S. X. He, Z. X. Wang, Y. Chen, and G. Hu, *Appl. Phys. Lett.* **84**, 2901 (2004).
- <sup>23</sup>X. Xiao, J. W. Elam, S. Trasobares, O. Auciello, and J. A. Carlisle, *Adv. Mater.* **17**, 1496 (2005).
- <sup>24</sup>C. Hébert, J. P. Mazellier, E. Scorsone, M. Mermoux, and P. Bergonzo, *Carbon* **71**, 27 (2014).
- <sup>25</sup>C. S. Wang, H. C. Chen, H. F. Cheng, and I. N. Lin, *Diamond Relat. Mater.* **18**, 136 (2009).
- <sup>26</sup>H. F. Cheng, H. Y. Chiang, C. C. Horng, H. C. Chen, C. S. Wang, and I. N. Lin, *J. Appl. Phys.* **109**, 033711 (2011).
- <sup>27</sup>T. H. Chang, K. Panda, B. K. Panigrahi, S. C. Lou, C. Chen, H. C. Chan, I. N. Lin, and N. H. Tai, *J. Phys. Chem. C* **116**, 19867 (2012).
- <sup>28</sup>Y. P. Raizer, *Gas Discharge Physics* (Springer-Verlag, New York, 1991).
- <sup>29</sup>R. H. Fowler and L. Nordheim, *Proc. R. Soc. London, Ser. A* **119**, 173 (1928).
- <sup>30</sup>T. H. Chang, S. Kunuku, K. C. Leou, N. H. Tai, and I. N. Lin, High stability of electron field emission behavior of carbon nanotubes by coating ultrananocrystalline diamond films (private communication).
- <sup>31</sup>T. H. Chang, S. Kunuku, K. C. Leou, N. H. Tai, and I. N. Lin, ACS Appl. Mater. Interfaces; Enhancement on the stability of electron field emission behavior and the related microplasma devices of carbon nanotubes by coating diamond films (private communication).